

Possible Supercritical Accretion on the ULX in the Metal-poor Galaxy IZw 18

MARINA YOSHIMOTO ¹, TOMOKAGE YONEYAMA ², HIROFUMI NODA ³, HIROKAZU ODAKA ^{1,4,5} AND HIRONORI MATSUMOTO^{1,4}¹*Department of Earth and Space Science, Graduate School of Science, Osaka University, 1-1 Machikaneyama, Toyonaka, Osaka 560-0043, Japan*²*Department of Physics, Faculty of Science and Engineering, Chuo University, 1-13-27 Kasuga, Bunkyo-ku, Tokyo 112-8551, Japan*³*Astronomical Institute, Tohoku University, 6-3 Aramaki-zaaoba, Aoba-ku, Sendai, Miyagi 980-8578, Japan*⁴*Forefront Research Center, Graduate School of Science, Osaka University, 1-1 Machikaneyama, Toyonaka, Osaka 560-0043, Japan*⁵*Kavli Institute for the Physics and Mathematics of the Universe, The University of Tokyo, 5-1-5 Kashiwanoha, Kashiwa, Chiba, 277-8583, Japan*

ABSTRACT

We present an analysis of X-ray observations of the Ultraluminous X-ray source (ULX) in IZw 18 based on archival data taken with *Chandra*, *XMM-Newton*, and *Suzaku*. This ULX is considered to be an intermediate-mass black hole candidate simply because it is in the lowest metallicity environment among ULXs, where formation of heavy black holes is facilitated. However, actual study of the ULX based on observations spanning for a long period has been too limited to determine its nature. In this study, we investigate the spectral evolution of the ULX up to 2014, combining the previously-unpublished *Suzaku* data with those from the other two satellites. We derive a positive correlation of $L \propto T_{\text{in}}^{2.1 \pm 0.4}$ between the bolometric luminosity L and inner-disk temperature T_{in} on the basis of the multi-color disk-blackbody model, where we exclude the *Chandra* data, which has the lowest luminosity and systematic residuals in the fitting. The nominal relation $L \propto T_{\text{in}}^4$ for the standard disk is rejected at a significance level of 1.5%. These results suggest that the ULX was in the slim-disk state during these observations except at the time of the *Chandra* observation, in which the ULX was likely to be in a different state. The apparent inner-disk radius appears negatively correlated with the inner-disk temperature. Moreover, we find a radial dependence of the disk temperature of $T(r) \propto r^{-p}$ with $p < 0.75$, which also supports the hypothesis that the ULX has a slim disk. In consequence, the IZw 18 ULX is most likely to be powered by a stellar-mass compact object in supercritical accretion.

Keywords: Ultraluminous x-ray sources(2164) — X-ray transient sources(1852) — High mass x-ray binary stars(733) — Blue compact dwarf galaxies(165)

1. INTRODUCTION

Ultraluminous X-ray sources (ULXs) are generally known to be non-nuclear, point-like objects observed in external galaxies. In particular, the most distinctive feature is a soft X-ray (0.3 – 10 keV) luminosity of $L_{\text{X}} \gtrsim 10^{39} \text{ erg s}^{-1}$, which exceeds the Eddington limit for stellar-mass black holes (BHs) of $10 M_{\odot}$, under an assumption of isotropic emission (see reviews by Feng & Soria 2011; Kaaret et al. 2017; King et al. 2023). The discovery of ULXs was made with the *Einstein* Observatory (Fabbiano 1989), and 1843 candidates, according to Walton et al. (2022), are known by now. The soft

X-ray spectra of ULXs are typically reproduced with a model of multi-color disk blackbody (MCD) and Comptonization components, as observed in Galactic black hole X-ray binaries (GBHBs). However, the presence of a spectral cutoff above 10 keV in ULX spectra (Bachetti et al. 2013) is a distinctively different feature from GBHBs. The luminosity of an accretion disk strongly depends on the mass and mass accretion rate of the object. Accordingly, the ultra-high luminosity of ULXs, much higher than that of GBHBs, is usually hypothesized with either or both massive central objects and/or supercritical accretion.

The earliest theories proposed that ULXs were a population of intermediate-mass black holes (IMBHs) with sub-Eddington accretion (Colbert & Mushotzky 1999; Makishima et al. 2000). For instance, ESO 243-49 HLX-

1, one of the so-called hyper-luminous X-ray sources, which are the ULX population defined with a luminosity of $L_X \gtrsim 10^{41} \text{ erg s}^{-1}$ (Matsumoto et al. 2003), has been an IMBH candidate on the basis of the relation between luminosity and inner-disk temperature consistent with a standard disk property of $L_{\text{bol}} \propto T_{\text{in}}^4$, where L_{bol} is a bolometric luminosity (Shakura & Sunyaev 1973), at a luminosity of $\sim 10^{42} \text{ erg s}^{-1}$. However, the discovery of pulsation (Bachetti et al. 2014) and ultrafast ($\sim 0.2c$) outflows (Pinto et al. 2016, 2017) in some ULXs suggests that stellar-mass BHs or neutron stars (NSs) with accretion in the super-Eddington mode are also candidate ULXs. Therefore, sub-Eddington accreting source is not the only nature of ULXs. ULXs are simply defined by the observed luminosity, and Bachetti (2016) suggested that a population of ULXs is in fact a “zoo” with a variety of species.

The majority of ULXs are found in spiral and irregular galaxies with high star-formation rates (SFRs; e.g., Irwin et al. 2004). The number of ULXs in a galaxy normalized by the SFR is anti-correlated with metallicity (Pakull & Mirioni 2002; Mapelli et al. 2010, 2011; Prestwich et al. 2013). In the early universe, which had zero metallicity, deficiency of heavy elements is thought to facilitate forming of massive stars (Population III; e.g., Hirano et al. 2014). The massive stars eventually become heavy BHs (e.g., Belczynski et al. 2010). The environment also facilitates accretion of Roche-lobe overflow type onto compact objects in binary systems (Linden et al. 2010). For these reasons, it may be possible that ULXs evolved in low metallicity galaxies are driven by IMBHs in sub-Eddington accretion (Zampieri & Roberts 2009; Mapelli et al. 2010). Wiktorowicz et al. (2017) proposed that the nature of ULXs is expected to differ depending on the star formation history of their host galaxies. If the SFR does not vary over time in low metallicity environments, BH ULXs are more abundant than NS ULXs during 10 Gyr since the beginning of star formation in the Universe. Conversely, if a burst of star-formation occurred in the first 100 Myr, NS ULXs should have outnumbered BH ULXs within $\lesssim 1$ Gyr and have become dominant after a few Gyr, regardless of the metallicity. Determining the nature of the ULX in metal-poor galaxies is crucial for delving into the evolution of binary systems.

Blue Compact Dwarf galaxies (BCDs) are the least chemically evolved galaxies in the local universe (Thuan & Martin 1981), which has an extraordinarily low metallicity of $1/50 - 1/3 Z_{\odot}$ (see, e.g., the review by Kunth & Östlin 2000). Kaaret et al. (2011) revealed the total X-ray luminosity of four X-ray point sources in three BCDs is 10 times larger than that of star-forming galax-

ies with normal metallicity. The finding suggests that the low metallicity environment is closely related to the evolution of X-ray sources.

IZwicky 18 (IZw 18; Zwicky 1966) is an extreme galaxy in BCDs. Optical spectroscopy found that the amount of oxygen was $12 + \log(\text{O}/\text{H}) = 7.11 \pm 0.01$ as a representative value (Kehrig et al. 2016). Comparing this with the solar value of $12 + \log(\text{O}/\text{H}) = 8.69 \pm 0.05$ (Asplund et al. 2009), the abundance of $Z = 0.026 Z_{\odot}$ is derived. Previously, IZw 18 had been thought to be composed of young systems that started star-formation only 500 Myr ago (Hunt et al. 2003; Izotov & Thuan 2004). However, Aloisi et al. (2007) indicated on the basis of deep HST/ACS photometry that IZw 18 contains old stars (≥ 1 Gyr), the fact of which implies that star formation started at $z \geq 0.1$. The distance for IZw 18 was obtained as $18.2 \pm 1.5 \text{ Mpc}$ and $19.0_{-2.5}^{+2.8} \text{ Mpc}$ from tip of red giant branch (Aloisi et al. 2007) and Cepheids (Fiorentino et al. 2010; Marconi et al. 2010), respectively. We adopted the distance of 18.2 Mpc in this work as well as previous works (Kaaret & Feng 2013; Lebouteiller et al. 2017; Kehrig et al. 2021).

IZw 18 contains an ULX located at R.A. = $09^{\text{h}}34^{\text{m}}02^{\text{s}}.0$, DEC. = $+55^{\circ}14'28''.0$ (J2000.0). In the past decades, X-ray spectral modeling of the ULX was carried out in several previous works. Fourniol et al. (1996) showed the X-ray source has a luminosity of $6.2_{-4.9}^{+2.3} \times 10^{39} \text{ erg s}^{-1}$ in the energy range of $0.1 - 2.4 \text{ keV}$, using ROSAT/PSPC data. Martin (1996) also used ROSAT/PSPC data and reported a luminosity of $\approx 1 \times 10^{39} \text{ erg s}^{-1}$ to within a factor of two accounting for the Galactic absorption. Bomans & Weis (2002) confirmed that the Chandra/ACIS-S data in 2000 was well fitted with a power-law model. Thuan et al. (2004) reported a luminosity of $1.6 \times 10^{39} \text{ erg s}^{-1}$ from the power-law model fitting with the Chandra/ACIS-S data in the energy range of $0.5 - 10 \text{ keV}$. The first application of the MCD model, beyond the simple power-law model, to the ULX was made by Kaaret & Feng (2013) with the XMM-Newton/EPIC data in 2002. They found a luminosity exceeding $10^{40} \text{ erg s}^{-1}$ in the energy range of $0.3 - 10 \text{ keV}$ and interpreted the change in luminosity from the Chandra observation as a hard-to-soft transition between the two observations. Comparing the maximum luminosities of GBHBs in the hard state with the luminosity in the Chandra observation, the mass of the ULX was estimated to be $> 85 M_{\odot}$, suggesting that it is an IMBH. Kehrig et al. (2021) applied a power-law model to the ROSAT/PSPC, Chandra/ACIS-S, XMM-Newton/EPIC, and Swift/XRT data taken from 1992 to 2012. They reported that the luminosity of the X-ray source varied on timescales from days to years.

As stated above, the ULX, in the metal-poor galaxy IZw 18, was suggested to be an IMBH candidate. However, there was no study on the nature based on observations spanning for a long period. In this study, we investigate the long-term spectral evolution of the ULX in IZw 18 up to 2014, analyzing the previously-unpublished *Suzaku*/XIS data taken in two occasions in 2014 and combining them to the previously published data. *Suzaku*/XIS observed the IZw 18 ULX twice in 2014 with exposures of 17.3 ks and 82.1 ks. The second one of which is the longest single observation of this ULX ever made in X-rays. The *ROSAT*/PSPC and *Swift*/XRT data are excluded from the analysis due to insufficient photon statistics. We focus on disk radiation and examine variations in luminosity, inner-disk temperature, apparent inner-disk radius, and the radial dependence of disk temperature to investigate the nature of the ULX.

2. OBSERVATIONS AND DATA REDUCTION

We use five archival data sets made with *Chandra*/ACIS-S, *XMM-Newton*/EPIC, and *Suzaku*/XIS. The details of the observations are listed in Table 1.

The IZw 18 ULX is situated adjacent to a quasi-stellar object (QSO; 2CXO J093359.3+551550 in *Chandra* source Catalog version 2.0 Evans et al. 2020) and an active galactic nucleus (AGN; [AGG2006] 59 in *Sloan Digital Sky Survey* XMM-Newton AGN Spectral Properties Catalog, Akylas et al. 2006) on the celestial plane (Figure 1). They are potential contamination sources. We thus excluded them in the analysis of the *Suzaku* data.

2.1. *Chandra*

IZw 18 was observed with *Chandra* Advanced CCD Imaging Spectrometer (ACIS) -S with an exposure of 40.8 ks in the FAINT mode on 2000 February 8 to 9 (ObsID: 805, Sequence number: 600108, PI: Bomans, Epoch: C1). Data reduction was carried out using the *Chandra* Interactive Analysis of Observation software package (CIAO; Fruscione et al. 2006) version 4.14.0 with the *Chandra* X-ray Calibration Database (CALDB) files version 4.9.8. The downloaded data was reprocessed with the task `chandra_repro`. We extracted the image with the task `dmcopy` and assigned source and background regions as a circular region with a radius of $5''$ and an annulus with radii of $5'' - 30''$, respectively. The spectra, a photon redistribution matrix file (RMF), and an ancillary response file (ARF) were created us-

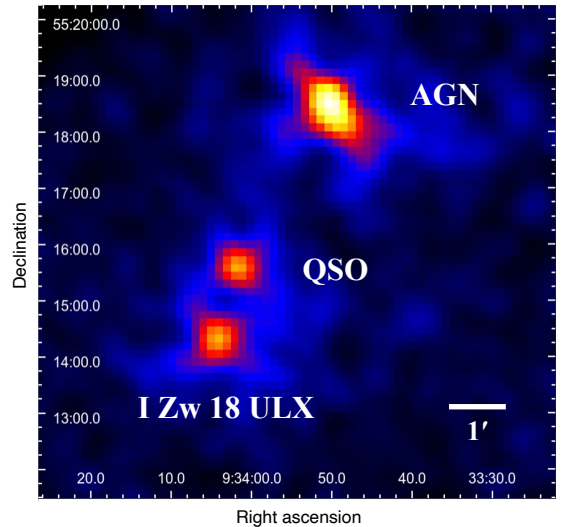


Figure 1. *Suzaku*/XIS0 image at epoch S2 around the IZw 18 ULX in the energy range of 0.5 – 7 keV. On the celestial plane, a QSO and AGN are located $1.4'$ and $5'$ away from the ULX, respectively. The angular distance between the ULX and QSO is shorter than the half-power diameter of *Suzaku* ($\sim 2'$), leading to contamination of photons between the two sources.

ing the task `specextract`. Our study identified background flaring in light curves generated with the task `dmextract`, as well as Thuan et al. (2004). However, the time regions that encompass background flaring are included in the following analysis because we found it does not significantly affect our results. The energy range for our spectral fitting is 0.4 – 10 keV.

2.2. *XMM-Newton*

We analyzed the archival data of two *XMM-Newton* observations in the Imaging mode on 2002 April 10 to 11 (ObsID: 0112520101; PI: Watson, Epoch: X1), and 2002 April 16 to 17 (ObsID: 0112520201; PI: Watson, Epoch: X2). The observation data of the pn, MOS1, and MOS2 detectors of the European Photon Imaging Camera (EPIC) were processed with the Science Analysis System (SAS) version 20.0.0 in the standard procedure. The calibration files of the March 2022 version were applied to the data with the tasks `epchain` and `emchain` for pn and MOS, respectively. We selected single and double events (`PATTERN<=4`) only for the pn and single, double, triple, and quadruple events (`PATTERN<=12`) only for the MOSs, with flags of `#XMMEA_EP && FLAG==0` and `#XMMEA_EM`, respectively. The periods with prominent flaring particle-backgrounds were determined from the light curves generated with the task `evselect` for single events in the high energy range (10 – 12 keV for pn, > 10 keV for MOSs). With these high-background periods excluded, the resultant net exposure times for

Table 1. Observation details of the I Zw 18 ULX analyzed in this work

Epoch	Observatory	Date [YYYY-MM-DD]	ObsID/Sequence number	Instrument	Net exposure time [ks]	Count rate [counts ks ⁻¹]
C1	<i>Chandra</i>	2000-02-08	805/600108	ACIS-S	40.8	13.0 ± 0.6
X1	<i>XMM-Newton</i>	2002-04-10	0112520101	EPIC-pn	24.1	91.4 ± 2.1
				EPIC-MOS1	31.1	28.7 ± 1.0
				EPIC-MOS2	30.9	28.7 ± 1.0
X2	<i>XMM-Newton</i>	2002-04-16	0112520201	EPIC-pn	5.4	79.1 ± 4.1
				EPIC-MOS1	18.5	26.7 ± 1.8
				EPIC-MOS2	18.6	28.0 ± 1.8
S1	<i>Suzaku</i>	2014-05-15	709021010	XIS0 + XIS3	17.3 + 17.3	4.2 ± 0.4
				XIS1	17.3	4.4 ± 0.8
S2	<i>Suzaku</i>	2014-10-04	709021020	XIS0 + XIS3	82.1 + 82.1	2.5 ± 0.1
				XIS1	82.1	2.4 ± 0.3

NOTE— Table columns from left to right: the name of epoch, observatory, observation start date, observation ID or sequence number, instrument, net exposure time, and count rate. In calculating the net exposure time, the periods with prominent flaring particle backgrounds are removed. The net exposure times of the EPIC-MOS data at epoch X2 are the sum of scheduled and unscheduled times.

pn, MOS1, and MOS2 were, respectively, 24.1, 31.1, and 30.9 ks in epoch X1, and 5.4, 18.5, and 18.6 ks in epoch X2. After these time-filtering, we extracted the images and spectra with the task `evselect`. The source regions for our analyses were a 30''-radius circle for each detector. The background regions for pn were three regions on the CCD chip encompassing the source, two circular regions of a 30''-radius (east and west) and a circular region with a radius of 70'' (south). Those for MOSs were, from an annulus region with radii of 30'' – 180'' excluding the 30''-radius circle centered at the QSO. In the MOS1 and MOS2 data in epoch X2, the spectra for the scheduled and unscheduled observations were extracted separately. We created RMFs and ARFs for each observation using the tasks `rmfgen` and `arfgen`, respectively. The spectral energy range is 0.2 – 10 keV.

2.3. *Suzaku*

Two pointing observations with *Suzaku* were made with the X-ray Imaging Spectrometers (XIS) 0, 1, and 3 on 2014 May 15 (ObsID: 709021010; PI: Kaaret, Epoch: S1) and 2014 October 4 to 5 (ObsID: 709021020; PI: Kaaret, Epoch: S2). For epoch S1, there were only 3 × 3 cleaned events for each detector with an exposure time of 17.3 ks. For epoch S2, we added 5 × 5 events to 3 × 3 events, resulting in a total exposure time of 82.1 ks for each detector. Images were extracted using the task `xselect` in HEASoft ([Nasa High Energy Astrophysics Science Archive Research Center \(Heasarc\) 2014](#)) version 6.30.1.

In the images, we found that the positions of the ULX, QSO, and AGN were shifted in the same direction from the catalog value. The typical positional uncertainty of *Suzaku* is 19'' ([Uchiyama et al. 2008](#)). We corrected the celestial positions of objects based on the cataloged position of the AGN. The source spectra were accumulated from a circular region of 41''-radius, using the task `xselect`. The background spectra were accumulated from an annular region of 2' to 6' radii centered at the middle position between the ULX and QSO, where a circular region of 1'8-radius centered at the AGN was excluded.

The RMFs were created with the task `xismrfgen` and the ARFs were, with the task `xissimarfgen` ([Ishisaki et al. 2007](#)) with CALDB files of the October 2018 version. The ULX and QSO are only 1/4 apart on the celestial plane. Given that the X-ray telescope (XRT) has a half-power diameter (HPD) of ~ 2' ([Serlemitsos et al. 2007](#)), the contamination from the QSO source due to the point spread function is significant and hence should be taken into account when analyzing the ULX data. The fraction of the photons leaking from the ULX and QSO into each other was reproduced through creating ARFs for ULX and QSO. For the front illuminated CCDs, XIS0 and XIS3, the spectra were summed together using the task `mathpha`, and response files were compiled by weighting the exposure time. We made simultaneous model fitting with the spectra of ULX and QSO in the energy range of 0.5 – 10 keV.

3. ANALYSIS AND RESULTS

The spectra are grouped into a minimum of 20 counts per energy bin using the HEASoft task `grppha`, the CIAO task `specextract`, and the SAS task `specgroup` for *Suzaku*, *Chandra*, and *XMM*, respectively. Simultaneous spectral model-fitting is performed with χ^2 statistics for the spectra of all the detectors in each epoch, in which the background is subtracted, using XSPEC version 12.12.1 (Arnaud 1996). In this section, the quoted errors of fitting parameters are in a 90% confidence level unless mentioned otherwise.

We estimate the Galactic absorption value to be $N_{\text{H}} = 2.92 \times 10^{20} \text{ cm}^{-2}$, using the HEASoft task `nh` (HI4PI

Collaboration et al. 2016) and convolve it as the `TBabs` model in XSPEC. The absorption intrinsic to the ULX is represented with the `TBvarabs` model and is free to vary with fixed parameter values of an abundance of $Z = 0.026 Z_{\odot}$ and a redshift of $z = 0.00254$. The spectral fitting results are listed in Table 2. All the data spectra, best-fit models, and residuals between them are shown in Figures 2 and 3. In the case of the *Suzaku* data, the IZw 18 ULX and QSO spectra are fitted simultaneously, and then the QSO spectra are reproduced with a power-law model.

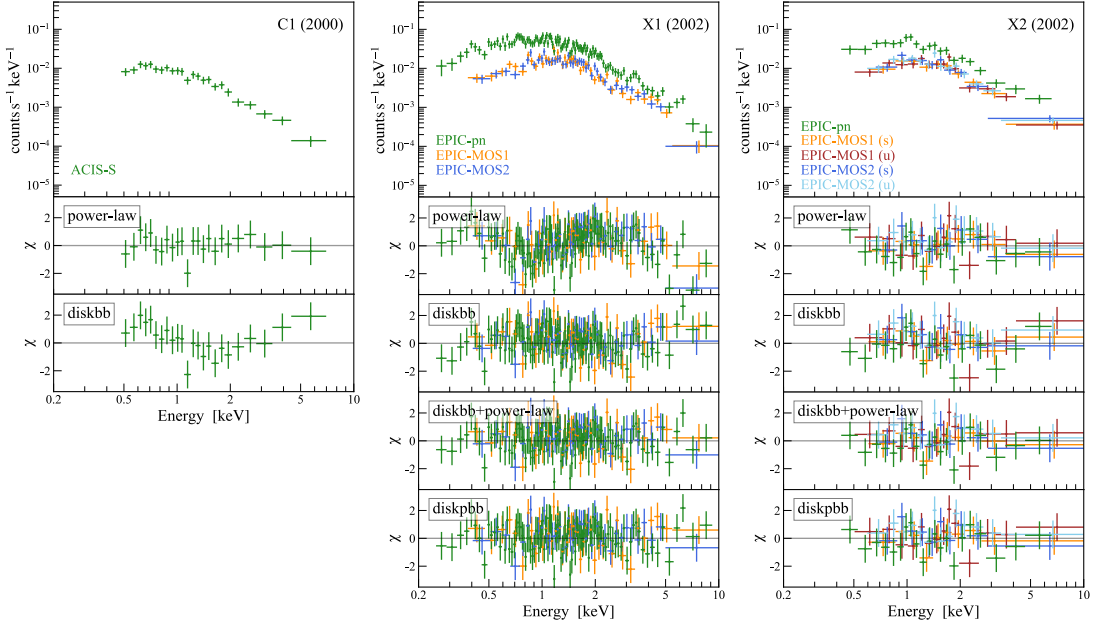


Figure 2. The 0.2 – 10 keV spectra of epochs C1, X1, and X2 for the IZw 18 ULX. Each data point is plotted with an error in 1σ confidence level. The χ ($= \text{data} - \text{model}/\text{error}$) distributions for absorbed models of `powerlaw`, `diskbb`, `diskbb+powerlaw`, and `diskpbb` (if applied) are shown in the lower panels below the spectra. For the EPIC-MOS1 and MOS2 data in epoch X2, the data in the scheduled (labeled as (s)) and unscheduled (u) periods are treated as the separate spectral data sets and are fitted simultaneously in combination with the pn data.

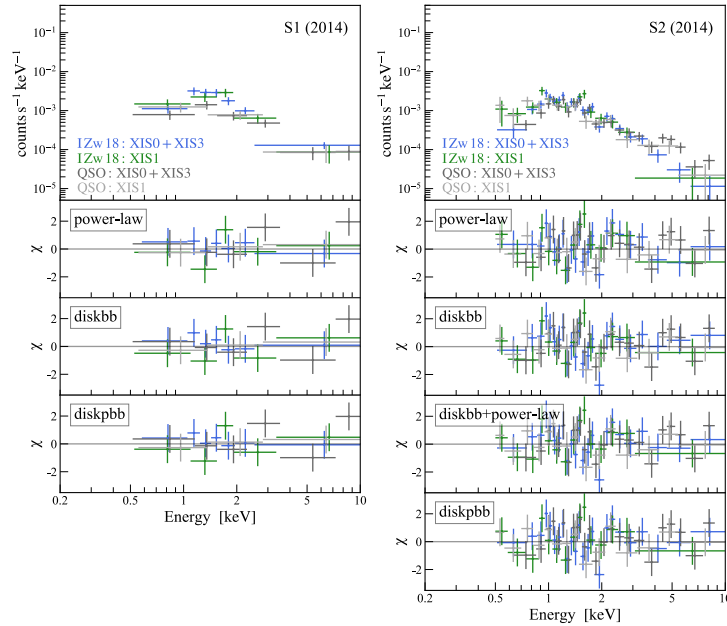


Figure 3. The same as in Figure 2 but with the *Suzaku*/XIS data in epochs S1 and S2, the data of which have never been published before. The IZw 18 ULX and QSO are 1.4 apart on the celestial plane, the distance of which is smaller than the *Suzaku* HPD.

Table 2. Results of spectral fitting for the IZw 18 ULX

Model	N_{H} [10^{21} cm^{-2}]	Γ	kT_{in} [keV]	p	$Norm_{\text{disk}}$	$Norm_{\text{Comp}}$	$f_{0.3-10 \text{ keV}}$ [$10^{-13} \text{ erg s}^{-1} \text{ cm}^{-2}$]	$L_{0.3-10 \text{ keV}}$ [$10^{39} \text{ erg s}^{-1}$]	$\chi^2/d.o.f.$
(1)	(2)	(3)	(4)	(5)	(6)	(7)	(8)	(9)	(10)
<i>Chandra</i> (2000-02-08)									
diskbb	< 0.88	—	$0.91^{+0.15}_{-0.14}$	—	$4.6^{+3.5}_{-1.8} \times 10^{-3}$	—	0.62	2.5	26.5/21
powerlaw	< 7.0	$1.9^{+0.2}_{-0.2}$	—	—	—	$1.5^{+0.2}_{-0.2} \times 10^{-5}$	0.94	3.7	9.40/21
<i>XMM1</i> (2002-04-10)									
diskbb	$2.7^{+1.0}_{-0.8}$	—	$1.1^{+0.0}_{-0.1}$	—	$1.0^{+0.2}_{-0.2} \times 10^{-2}$	—	2.8	11	195.7/193
powerlaw	13^{+3}_{-1}	$2.0^{+0.1}_{-0.1}$	—	—	—	$7.1^{+0.5}_{-0.4} \times 10^{-5}$	4.0	16	249.6/193
diskbb+powerlaw	$5.4^{+2.9}_{-2.4}$	$1.7^{+0.7}_{-1.0}$	$1.0^{+0.2}_{-0.1}$	—	$9.4^{+7.8}_{-4.4} \times 10^{-3}$	$1.8^{+1.2}_{-1.5} \times 10^{-5}$	3.1	12	180.5/191
diskpbb	$6.0^{+2.1}_{-1.8}$	—	$1.3^{+0.2}_{-0.1}$	$0.62^{+0.05}_{-0.04}$	$2.4^{+2.4}_{-1.2} \times 10^{-3}$	—	3.1	12	182.6/192
<i>XMM2</i> (2002-04-16)									
diskbb	< 4.0	—	$1.2^{+0.1}_{-0.1}$	—	$7.3^{+2.9}_{-2.1} \times 10^{-3}$	—	2.6	11	58.3/66
powerlaw	15^{+5}_{-4}	$1.9^{+0.2}_{-0.1}$	—	—	—	$6.7^{+0.9}_{-0.7} \times 10^{-5}$	4.0	16	50.7/66
diskbb+powerlaw	$8.2^{+9.1}_{-6.9}$	< 3.5	$0.83^{+1.10}_{-0.28}$	—	$1.0^{+3.8}_{-1.0} \times 10^{-2}$	$3.4^{+3.1}_{-3.4} \times 10^{-5}$	3.4	13	47.3/64
diskpbb	10^{+7}_{-5}	—	$1.9^{+5.1}_{-0.5}$	$0.56^{+0.07}_{-0.05}$	< 2.0×10^{-3}	—	< 3.4	< 13	48.0/65
<i>Suzaku 1</i> (2014-05-15)									
diskbb	< 47	—	$0.87^{+0.22}_{-0.19}$	—	$1.9^{+3.7}_{-1.2} \times 10^{-2}$	—	2.2	8.6	12.8/15
powerlaw	61^{+47}_{-31}	$2.7^{+0.5}_{-0.5}$	—	—	—	$1.1^{+0.8}_{-0.4} \times 10^{-4}$	5.3	21	13.0/15
diskpbb	< 73	—	$1.1^{+1.0}_{-0.4}$	(not constrained)	$2.4^{+52.5}_{-2.3} \times 10^{-3}$	—	3.1	12	12.5/14
<i>Suzaku 2</i> (2014-10-04)									
diskbb	< 8.4	—	$0.70^{+0.08}_{-0.10}$	—	$2.2^{+2.1}_{-0.8} \times 10^{-2}$	—	1.1	4.3	77.7/72
powerlaw	30^{+16}_{-13}	$2.9^{+0.3}_{-0.3}$	—	—	—	$5.7^{+1.7}_{-1.3} \times 10^{-5}$	2.9	11	77.0/72
diskbb+powerlaw	< 14	1.7 (fixed)	$0.63^{+0.13}_{-0.16}$	—	$3.0^{+6.7}_{-1.5} \times 10^{-2}$	< 9.4×10^{-6}	1.4	5.4	76.6/71
diskpbb	< 23	—	$0.96^{+0.28}_{-0.27}$	< 0.73	$1.9^{+19.7}_{-1.3} \times 10^{-3}$	—	1.6	6.5	74.9/71

NOTE—Best-fit parameters for each model with errors in the 90% confidence level in 5 epochs.

- (1) Model name in XSPEC. (2) Specific absorption column density in the ULX. (3) Photon index of the Comptonization component. (4) Inner-disk temperature of the disk component. (5) Index of the disk radial dependence of temperature, $T(r) \propto r^{-p}$. (6) Normalization for the disk component, as $r_{\text{in}}^2 \cos i / D_{10}^2$. (7) Normalization for the Comptonization component, as photons $\text{keV}^{-1} \text{cm}^{-2} \text{s}^{-1}$ at 1 keV. (8) Model flux in the energy range 0.3 – 10 keV. (9) Luminosity calculated multiplication of the 0.3 – 10 keV model flux and $4\pi \times (\text{distance})^2$. (10) Chi-square value of model fitting and the degree of freedom.

We apply a few models to model fitting of the IZw 18 ULX spectra. First, we apply the simple MCD model (TBabs*TBvarabs*diskbb in XSPEC; Mitsuda et al. 1984; Makishima et al. 1986). The model is composed of two parameters: an inner-disk temperature kT_{in} [keV] and a normalization, $r_{\text{in}}^2 \cos i / D_{10}^2$, where r_{in} [km] is the apparent inner-disk radius, i is the inclination angle, and D_{10} [10 kpc] is the distance to the object. We find that the MCD model is rejected for none of the spectra at a significance level of 1%. The inner-disk temperature shows time variation; the highest is $1.2^{+0.1}_{-0.1}$ keV in epoch X2 and the lowest, $0.70^{+0.08}_{-0.10}$ keV in epoch S2. The determined unabsorbed luminosity for any of the spectra exceeds the ULX threshold of 10^{39} erg s $^{-1}$ in the energy range of 0.3 – 10 keV. The unabsorbed luminosity increased by a factor of about four, from 2.5×10^{39} erg s $^{-1}$ in 2000 (*Chandra* observation) to 11×10^{39} erg s $^{-1}$ in 2002 (*XMM-Newton* observations), and thus we confirm the previously-reported results (Kaaret & Feng 2013). The observations in epochs S1 and S2 in 2014 show luminosities of 8.6×10^{39} erg s $^{-1}$ and 4.3×10^{39} erg s $^{-1}$, respectively, both of which are lower than those in the *XMM-Newton* observations in 2002.

Kaaret & Feng (2013) argued that the increase in the ULX luminosity between 2000 and 2002 was due to a hard-to-soft state transition of the ULX source. Indeed, fitting the data with a simple power-law model (TBabs*TBvarabs*powerlaw in XSPEC) shows that the model is rejected for only the data in epoch *XMM1*, which has the highest data quality among our data sets, at a significance level of 1%. By contrast, the chi-square value of the *Chandra* data is improved with the power-law model ($\chi^2/d.o.f = 9.40/21$) from the MCD model ($\chi^2/d.o.f = 26.5/21$). Although the MCD model is not rejected at a significance level of 1% with the *Chandra* data, the data show distinct systematic residuals (Figure 2). Thus, our results support the hypothesis of the ULX state transition between 2000 and 2002.

The spectra of most ULXs are known to be reproducible with dual-continuum models that combine two of the following models: a blackbody, a MCD, a MCD with power-law dependence for the temperature (diskpbb in XSPEC; e.g., Mineshige et al. 1994), a (cutoff) power-law, and a thermal Comptonization component (e.g., Middleton et al. 2015; Pintore et al. 2017; Koliopoulos et al. 2017; Walton et al. 2018). We then test the dual-continuum model with the IZw 18 ULX data. A simple MCD + power-law model (TBabs*TBvarabs*(diskbb+powerlaw) in XSPEC) is employed here because of the insufficient photon statistics, especially in the hard band (> 2 keV). The parameters are found to be meaningfully constrained only

with the good-statistics data of epochs X1, X2, and S2. We note that in the fitting for epoch S2 data, the photon index of the power-law model is fixed at the best-fit value of the fitting of the X1 data. The inner-disk temperatures are obtained to be $1.0^{+0.2}_{-0.1}$, $0.83^{+1.10}_{-0.28}$, and $0.63^{+0.13}_{-0.16}$ keV for epoch X1, X2, and S2 data, respectively. These values are almost the same as those determined with the single MCD model fitting for each observation. This result suggests that the spectra are not dominated by the power-law component.

We next explore a disk radial dependence of temperature $T(r) \propto r^{-p}$, where p is a free parameter in the diskpbb model (TBabs*TBvarabs*diskpbb in XSPEC). We obtain $kT_{\text{in}} = 1.3^{+0.2}_{-0.1}$, $1.9^{+5.1}_{-0.5}$, and $0.96^{+0.28}_{-0.27}$ keV and $p = 0.62^{+0.05}_{-0.04}$, and $0.56^{+0.07}_{-0.05}$, < 0.73 for epoch X1, X2, and S2 data, respectively. The obtained temperature kT_{in} is somewhat higher than those based on the other models. For the *Suzaku* 1 data, kT_{in} is poorly constrained, $1.1^{+1.0}_{-0.4}$ keV, and p is not constrained. The *Chandra* data have inadequate statistics to yield significant results.

4. DISCUSSION

We discuss the time variation of the inner-disk temperature kT_{in} with the MCD model. The best-fit value of kT_{in} is in a range of 0.7 – 1.2 keV. We here investigate a temperature dependence on the bolometric luminosity through a long-term spectral evolution. For the standard disk—optically thick and geometrically thin—where a half of the gravitational potential energy is converted into blackbody radiation, the luminosity follows $L_{\text{bol}} \propto T_{\text{in}}^4$ (Shakura & Sunyaev 1973). As the accretion rate increases, the slim disk—optically and geometrically thick—appears, where advection decreases the radiation efficiency, and the luminosity relation approaches $L_{\text{bol}} \propto T_{\text{in}}^2$ (Abramowicz et al. 1988; Watarai et al. 2000; Watarai & Mineshige 2001). Figure 4 plots the obtained data points on the $L - kT_{\text{in}}$ space, where the luminosity in an energy range of 0.1 – 50 keV is regarded as the bolometric luminosity L . We discuss the relation with χ^2 test. Using all the data, the luminosity relation model for the standard disk, $L \propto T_{\text{in}}^4$, is rejected at a significance level of 1%. Also, that for the slim disk of $L \propto T_{\text{in}}^2$ is rejected at a significance level of 1%. The slim disk is expected to appear at a high Eddington ratio according to the standard model. For this reason, we then exclude the *Chandra* data, which has the lowest luminosity in our data sets and shows apparent systematic residuals in our fitting result with the diskbb model, and re-evaluate the above-mentioned relations. The evaluation shows that at a significance level of 1.5%, $L \propto T_{\text{in}}^4$ is rejected, whereas $L \propto T_{\text{in}}^2$ is not. When the power-

law index in the relation is allowed to vary, the relation is derived to be $L \propto T_{\text{in}}^{2.1 \pm 0.4}$, which is consistent with the expected property of a slim disk with supercritical accretion. If the *Chandra* data is included in the fitting, the best-fit relation is $L \propto T_{\text{in}}^{3.2 \pm 0.6}$, but the fitting is rejected at a significance level of 1%. Here, these errors are evaluated with 1σ confidence intervals. These results suggest the hypothesis that most of the observations the data of which we have used in this work were performed when the ULX was in the slim disk state, and the *Chandra* observation was made when the ULX was in a different state from the others. The nature of the IZw 18 ULX may be a stellar-mass compact object.

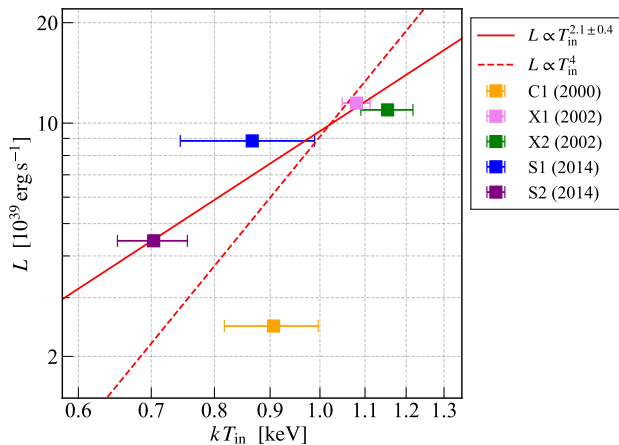


Figure 4. Relation between the bolometric luminosity L and inner-disk temperature kT_{in} . Error bars show the 1σ confidence intervals derived with the MCD model. The solid red line shows the best-fit relation of $L \propto T_{\text{in}}^{2.1 \pm 0.4}$, where the *Chandra* data are excluded from the fitting (see text for detail). The dashed red line shows the nominal relation of $L \propto T_{\text{in}}^4$ for the standard disk (Shakura & Sunyaev 1973).

We also investigate the relation between the apparent inner-disk radius and the inner-disk temperature. It should be noted that observed disk-blackbody spectra usually deviate from the MCD model due to inverse Compton scattering and a boundary condition at the innermost stable circular orbit (ISCO). Typically, the corrected apparent radius R_{in} for a standard disk is calculated according to $\xi \kappa^2 r_{\text{in}}$, using a boundary-condition correction factor of $\xi = \sqrt{\frac{3}{7}} \left(\frac{6}{7}\right)^3 \sim 0.41$ (Kubota et al. 1998) and a hardening factor for color-temperature correction of $\kappa \sim 1.7$ (Shimura & Takahara 1995). In Figure 5, we show the relation between the apparent radius R_{in} and the inner-disk temperature kT_{in} with our data, where we do not take into account the correction factor κ in our calculation because in the low metallicity environment, the effect of electron scattering (opac-

ity and Comptonization; Kawaguchi 2003) deviates from the typical value. The apparent radius appears to decrease as the temperature increases with our data. The *Chandra* data point appears to show a different trend from the other data. For the standard disk, an apparent radius is expected to be constant in a thermal state. When we fit the apparent radius with a constant model excluding the *Chandra* data, the model is rejected at a significance level of 7%, reinforcing the negative relation. The negative relation between R_{in} and T_{in} for ULXs were reported in several studies, $R_{\text{in}} \propto T_{\text{in}}^{-1}$ (Watarai et al. 2000; Mizuno et al. 2001) or $R_{\text{in}} \propto T_{\text{in}}^{-2}$ (Urquhart & Soria 2016; Soria & Kong 2016), for supercritical accretion. We overlay the two relations in Figure 5. The set of data of the IZw 18 ULX appear to match well the negative $R_{\text{in}} - T_{\text{in}}$ relation. This result is consistent with the ULX being driven by supercritical accretion with a stellar-mass compact object.

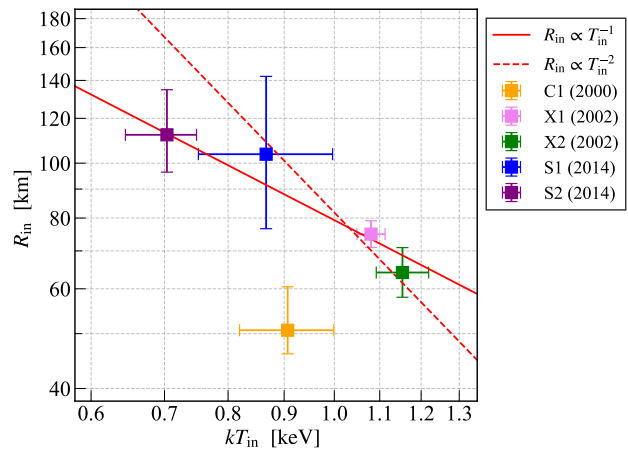


Figure 5. The apparent inner-disk radius R_{in} versus its temperature kT_{in} with 1σ confidence level. The *Chandra* data point seems to be an outlier. The radius R_{in} is not constant at a 7% significance level, where *Chandra* data point is excluded in the calculation. It appears to be consistent with the relations $R_{\text{in}} \propto T_{\text{in}}^{-1}$ (solid red line) or $R_{\text{in}} \propto T_{\text{in}}^{-2}$ (dashed red line) for supercritical accretion.

The strongest observational evidence for supercritical accretion is detection of emission and absorption lines originating in a fast outflow. They are highly redshifted or blueshifted in several ULXs (Pinto et al. 2016, 2017). Because the photon statistics are not enough, we see no clear emission or absorption lines in our spectra. Kajava & Poutanen (2009) classified 11 ULXs into three spectral types; the power-law dominant type, the MCD dominant type, which shows a positive $L - T_{\text{in}}$ correlation, and the cool MCD (0.1 – 0.3 keV) + power-law type, which shows a negative correlation of $L \propto T_{\text{in}}^{-3.5}$. In the negatively correlated case “outflow-dominated

ULXs”, the X-ray photons are believed to originate from the photosphere of the optically thick outflow (funnel), whose temperature decreases as the mass accretion rate increases (Poutanen et al. 2007). Indeed, a negative trend was found in NGC 1313 X-2, which is a pulsating neutron star in supercritical accretion (Feng & Kaaret 2007; Kajava & Poutanen 2009; Robba et al. 2021). In our study, the relation between the luminosity and temperature is derived to be $L \propto T_{\text{in}}^{1.7 \pm 0.7}$ (1σ confidence interval) from MCD + power-law model fitting. The inner-disk temperature of the IZw 18 ULX is higher (> 0.5 keV) than those of outflow-dominated ULXs. Therefore, we consider that the accretion disk is more predominant than the outflow in the IZw 18 ULX.

The spectral model fitting with the `diskpbb` model is an effective way to distinguish the disk states. The standard disk is reproduced with $p = 0.75$ (Shakura & Sunyaev 1973), whereas the p -value for the slim disk appears to approach $p = 0.50$ (Watarai & Fukue 1999; Watarai et al. 2000). For the IZw 18 ULX, the disk radial dependence of temperature is $p < 0.75$ for $T(r) \propto r^{-p}$. The value is significantly different from that for the standard disk. This result also reinforces the hypothesis that IZw 18 ULX is in supercritical accretion onto a stellar-mass compact object.

IZw 18 is thought to have begun star formation more than 1 Gyr ago (Aloisi et al. 2007). According to Wiktorowicz et al. (2017), if a SFR has been constant since the beginning of star formation in a low-metallicity environment, ULXs are likely to be BHs. On the contrary, if a burst star-forming occurred in the past, ULXs could be either BHs or NSs. With the limited photon statistics of the currently available X-ray observation data for the IZw 18 ULX, we cannot determine whether it is a BH or NS. In addition to spectral analysis, search for pulsation, quasi-periodic oscillation, or flat-topped noise (e.g., Atapin et al. 2019) with longer observations in the future will be useful to determine what the IZw 18 ULX actually is.

5. CONCLUSIONS

In this study, we investigate the spectral evolution of the ULX in metal-poor galaxy IZw 18 for fourteen years, using five observations from *Chandra*, *XMM-Newton*, and *Suzaku*. The inclusion of the data from two previously-unpublished *Suzaku* observations allows us to examine spectral parameter correlations. It also helps us to confirm that the *Chandra* observation was made when the source was in a different state from other epochs. We suggest that the IZw 18 ULX is driven with a supercritical accreting flow with a stellar-mass compact object based on the following findings:

1. The IZw 18 ULX shows a positive correlation between the bolometric luminosity L and the inner-disk temperature T_{in} , which we derive to be $L \propto T_{\text{in}}^{2.1 \pm 0.4}$ with the MCD model, where we exclude the *Chandra* data because the source state differed at the time of the *Chandra* observation. The relation $L \propto T_{\text{in}}^4$ for the standard disk is rejected at a significance level of 1.5%.
2. The apparent inner-disk radius R_{in} is not constant at a significance level of 7%, where the *Chandra* data are excluded in the estimate. The radius appears negatively correlated with the disk temperature in a similar way as previously suggested for some other ULXs with $R_{\text{in}} \propto T_{\text{in}}^{-1}$ or $R_{\text{in}} \propto T_{\text{in}}^{-2}$.
3. The radial dependence of the disk temperature is obtained to be $T(r) \propto r^{-p}$ with $p < 0.75$. This is consistent with the slim disk ($p \sim 0.5$) and differs from the standard disk ($p = 0.75$).

In general, low metallicity environments are considered to facilitate the formation of heavy BHs. It has been believed that IMBH ULXs are abundant in such environments. However, the ULX in metal-poor galaxy IZw 18 is a possible stellar-mass compact object. To determine the general nature of the ULX is essential for delving into the evolution of binary systems. Longer observations and systematic studies are needed to reveal what factors determine their nature.

We would like to thank the anonymous referee for his/her valuable comments and suggestions. This work was conducted with the late Dr. K. Hayashida. This research has made use of data obtained from the High Energy Astrophysics Science Archive Research Center (HEASARC), which is a service of the Astrophysics Science Division at NASA/GSFC, and the XMM-Newton Science Archive (XSA). This research also employs a Chandra dataset, obtained by the Chandra X-ray Observatory, contained in the Chandra Data Collection (CDC) 239 doi:10.25574/cdc.239. The data of *Suzaku* satellite, which is a collaborative mission between the space agencies of Japan (JAXA) and the NASA, the USA played an important role in this research. We use X-ray data analysis software of the application packages HEASoft, CIAO, and SAS provided by the HEASARC, the Chandra X-ray Center (CXC), and the ESA XMM Science Operations Centre (SOC), respectively. This work is supported by the Japan Science and Technology Agency (JST) Support for Pioneering Research Initiated by the Next Generation (SPRING) with Grant Number JPMJSP2138, the Japan Society for the Promotion of Science (JSPS) Grants-in-Aid for Scientific Research (KAKENHI) with Grant Numbers 19K21884, 20H00175, 20H00178, 20H01941, 20H01947, 20KK0071, 21K20372, 22H00128, 22K18277, and 23H00128, and the Toray Science and Technology Grant Number 20-6104 (Toray Science Foundation).

Facilities: CXO (ACIS), XMM (EPIC), Suzaku (XIS)

Software: HEASoft (Nasa High Energy Astrophysics Science Archive Research Center (Heasarc) 2014), CIAO (Fruscione et al. 2006), SAS, XSPEC (Arnaud 1996), SAOImageDS9 (Joye & Mandel 2003), numpy (Harris et al. 2020), scipy (Virtanen et al. 2020), matplotlib (Hunter 2007), astropy (Astropy Collaboration et al. 2013, 2018, 2022)

REFERENCES

- Abramowicz, M. A., Czerny, B., Lasota, J. P., & Szuszkiewicz, E. 1988, ApJ, 332, 646, doi: [10.1086/166683](https://doi.org/10.1086/166683)
- Akylas, A., Georgantopoulos, I., Georgakakis, A., Kitsionas, S., & Hatziminaoglou, E. 2006, A&A, 459, 693, doi: [10.1051/0004-6361:20054632](https://doi.org/10.1051/0004-6361:20054632)
- Aloisi, A., Clementini, G., Tosi, M., et al. 2007, ApJL, 667, L151, doi: [10.1086/522368](https://doi.org/10.1086/522368)
- Arnaud, K. A. 1996, in Astronomical Society of the Pacific Conference Series, Vol. 101, Astronomical Data Analysis Software and Systems V, ed. G. H. Jacoby & J. Barnes, 17
- Asplund, M., Grevesse, N., Sauval, A. J., & Scott, P. 2009, ARA&A, 47, 481, doi: [10.1146/annurev.astro.46.060407.145222](https://doi.org/10.1146/annurev.astro.46.060407.145222)
- Astropy Collaboration, Robitaille, T. P., Tollerud, E. J., et al. 2013, A&A, 558, A33, doi: [10.1051/0004-6361/201322068](https://doi.org/10.1051/0004-6361/201322068)
- Astropy Collaboration, Price-Whelan, A. M., Sipőcz, B. M., et al. 2018, AJ, 156, 123, doi: [10.3847/1538-3881/aabc4f](https://doi.org/10.3847/1538-3881/aabc4f)
- Astropy Collaboration, Price-Whelan, A. M., Lim, P. L., et al. 2022, ApJ, 935, 167, doi: [10.3847/1538-4357/ac7c74](https://doi.org/10.3847/1538-4357/ac7c74)
- Atapin, K., Fabrika, S., & Caballero-García, M. D. 2019, MNRAS, 486, 2766, doi: [10.1093/mnras/stz1027](https://doi.org/10.1093/mnras/stz1027)
- Bachetti, M. 2016, Astronomische Nachrichten, 337, 349, doi: [10.1002/asna.201612312](https://doi.org/10.1002/asna.201612312)
- Bachetti, M., Rana, V., Walton, D. J., et al. 2013, ApJ, 778, 163, doi: [10.1088/0004-637X/778/2/163](https://doi.org/10.1088/0004-637X/778/2/163)
- Bachetti, M., Harrison, F. A., Walton, D. J., et al. 2014, Nature, 514, 202, doi: [10.1038/nature13791](https://doi.org/10.1038/nature13791)
- Belczynski, K., Bulik, T., Fryer, C. L., et al. 2010, ApJ, 714, 1217, doi: [10.1088/0004-637X/714/2/1217](https://doi.org/10.1088/0004-637X/714/2/1217)
- Bomans, D. J., & Weis, K. 2002, in Astronomical Society of the Pacific Conference Series, Vol. 262, The High Energy Universe at Sharp Focus: Chandra Science, ed. E. M. Schlegel & S. D. Vrtilek, 141
- Colbert, E. J. M., & Mushotzky, R. F. 1999, ApJ, 519, 89, doi: [10.1086/307356](https://doi.org/10.1086/307356)

- Evans, I. N., Primini, F. A., Miller, J. B., et al. 2020, in American Astronomical Society Meeting Abstracts, Vol. 235, American Astronomical Society Meeting Abstracts #235, 154.05
- Fabbiano, G. 1989, *ARA&A*, 27, 87, doi: [10.1146/annurev.aa.27.090189.000511](https://doi.org/10.1146/annurev.aa.27.090189.000511)
- Feng, H., & Kaaret, P. 2007, *ApJL*, 660, L113, doi: [10.1086/518309](https://doi.org/10.1086/518309)
- Feng, H., & Soria, R. 2011, *NewAR*, 55, 166, doi: [10.1016/j.newar.2011.08.002](https://doi.org/10.1016/j.newar.2011.08.002)
- Fiorentino, G., Contreras Ramos, R., Clementini, G., et al. 2010, *ApJ*, 711, 808, doi: [10.1088/0004-637X/711/2/808](https://doi.org/10.1088/0004-637X/711/2/808)
- Fourniol, N., Pakull, M. W., & Motch, C. 1996, in *Roentgenstrahlung from the Universe*, ed. H. U. Zimmermann, J. Trümper, & H. Yorke, 375–376
- Fruscione, A., McDowell, J. C., Allen, G. E., et al. 2006, in *Society of Photo-Optical Instrumentation Engineers (SPIE) Conference Series*, Vol. 6270, Society of Photo-Optical Instrumentation Engineers (SPIE) Conference Series, ed. D. R. Silva & R. E. Doxsey, 62701V, doi: [10.1117/12.671760](https://doi.org/10.1117/12.671760)
- Harris, C. R., Millman, K. J., van der Walt, S. J., et al. 2020, *Nature*, 585, 357, doi: [10.1038/s41586-020-2649-2](https://doi.org/10.1038/s41586-020-2649-2)
- HI4PI Collaboration, Ben Bekhti, N., Flöer, L., et al. 2016, *A&A*, 594, A116, doi: [10.1051/0004-6361/201629178](https://doi.org/10.1051/0004-6361/201629178)
- Hirano, S., Hosokawa, T., Yoshida, N., et al. 2014, *ApJ*, 781, 60, doi: [10.1088/0004-637X/781/2/60](https://doi.org/10.1088/0004-637X/781/2/60)
- Hunt, L. K., Thuan, T. X., & Izotov, Y. I. 2003, *ApJ*, 588, 281, doi: [10.1086/368352](https://doi.org/10.1086/368352)
- Hunter, J. D. 2007, *Computing in Science & Engineering*, 9, 90, doi: [10.1109/MCSE.2007.55](https://doi.org/10.1109/MCSE.2007.55)
- Irwin, J. A., Bregman, J. N., & Athey, A. E. 2004, *ApJL*, 601, L143, doi: [10.1086/382026](https://doi.org/10.1086/382026)
- Ishisaki, Y., Maeda, Y., Fujimoto, R., et al. 2007, *PASJ*, 59, 113, doi: [10.1093/pasj/59.sp1.S113](https://doi.org/10.1093/pasj/59.sp1.S113)
- Izotov, Y. I., & Thuan, T. X. 2004, *ApJ*, 616, 768, doi: [10.1086/424990](https://doi.org/10.1086/424990)
- Joye, W. A., & Mandel, E. 2003, in *Astronomical Society of the Pacific Conference Series*, Vol. 295, *Astronomical Data Analysis Software and Systems XII*, ed. H. E. Payne, R. I. Jedrzejewski, & R. N. Hook, 489
- Kaaret, P., & Feng, H. 2013, *ApJ*, 770, 20, doi: [10.1088/0004-637X/770/1/20](https://doi.org/10.1088/0004-637X/770/1/20)
- Kaaret, P., Feng, H., & Roberts, T. P. 2017, *ARA&A*, 55, 303, doi: [10.1146/annurev-astro-091916-055259](https://doi.org/10.1146/annurev-astro-091916-055259)
- Kaaret, P., Schmitt, J., & Gorski, M. 2011, *ApJ*, 741, 10, doi: [10.1088/0004-637X/741/1/10](https://doi.org/10.1088/0004-637X/741/1/10)
- Kajava, J. J. E., & Poutanen, J. 2009, *MNRAS*, 398, 1450, doi: [10.1111/j.1365-2966.2009.15215.x](https://doi.org/10.1111/j.1365-2966.2009.15215.x)
- Kawaguchi, T. 2003, *ApJ*, 593, 69, doi: [10.1086/376404](https://doi.org/10.1086/376404)
- Kehrig, C., Guerrero, M. A., Vílchez, J. M., & Ramos-Larios, G. 2021, *ApJL*, 908, L54, doi: [10.3847/2041-8213/abe41b](https://doi.org/10.3847/2041-8213/abe41b)
- Kehrig, C., Vílchez, J. M., Pérez-Montero, E., et al. 2016, *MNRAS*, 459, 2992, doi: [10.1093/mnras/stw806](https://doi.org/10.1093/mnras/stw806)
- King, A., Lasota, J.-P., & Middleton, M. 2023, *NewAR*, 96, 101672, doi: [10.1016/j.newar.2022.101672](https://doi.org/10.1016/j.newar.2022.101672)
- Koliopanos, F., Vasilopoulos, G., Godet, O., et al. 2017, *A&A*, 608, A47, doi: [10.1051/0004-6361/201730922](https://doi.org/10.1051/0004-6361/201730922)
- Kubota, A., Tanaka, Y., Makishima, K., et al. 1998, *PASJ*, 50, 667, doi: [10.1093/pasj/50.6.667](https://doi.org/10.1093/pasj/50.6.667)
- Kunth, D., & Östlin, G. 2000, *A&A Rv*, 10, 1, doi: [10.1007/s001590000005](https://doi.org/10.1007/s001590000005)
- Lebouteiller, V., Péquignot, D., Cormier, D., et al. 2017, *A&A*, 602, A45, doi: [10.1051/0004-6361/201629675](https://doi.org/10.1051/0004-6361/201629675)
- Linden, T., Kalogera, V., Sepinsky, J. F., et al. 2010, *ApJ*, 725, 1984, doi: [10.1088/0004-637X/725/2/1984](https://doi.org/10.1088/0004-637X/725/2/1984)
- Makishima, K., Maejima, Y., Mitsuda, K., et al. 1986, *ApJ*, 308, 635, doi: [10.1086/164534](https://doi.org/10.1086/164534)
- Makishima, K., Kubota, A., Mizuno, T., et al. 2000, *ApJ*, 535, 632, doi: [10.1086/308868](https://doi.org/10.1086/308868)
- Mapelli, M., Ripamonti, E., Zampieri, L., & Colpi, M. 2011, *Astronomische Nachrichten*, 332, 414, doi: [10.1002/asna.201011511](https://doi.org/10.1002/asna.201011511)
- Mapelli, M., Ripamonti, E., Zampieri, L., Colpi, M., & Bressan, A. 2010, *MNRAS*, 408, 234, doi: [10.1111/j.1365-2966.2010.17048.x](https://doi.org/10.1111/j.1365-2966.2010.17048.x)
- Marconi, M., Musella, I., Fiorentino, G., et al. 2010, *ApJ*, 713, 615, doi: [10.1088/0004-637X/713/1/615](https://doi.org/10.1088/0004-637X/713/1/615)
- Martin, C. L. 1996, *ApJ*, 465, 680, doi: [10.1086/177453](https://doi.org/10.1086/177453)
- Matsumoto, H., Tsuru, T. G., Watari, K., Mineshige, S., & Matsushita, S. 2003, in *Astronomical Society of the Pacific Conference Series*, Vol. 289, *The Proceedings of the IAU 8th Asian-Pacific Regional Meeting*, Volume 1, ed. S. Ikeuchi, J. Hearnshaw, & T. Hanawa, 291–294
- Middleton, M. J., Walton, D. J., Fabian, A., et al. 2015, *MNRAS*, 454, 3134, doi: [10.1093/mnras/stv2214](https://doi.org/10.1093/mnras/stv2214)
- Mineshige, S., Hirano, A., Kitamoto, S., Yamada, T. T., & Fukue, J. 1994, *ApJ*, 426, 308, doi: [10.1086/174065](https://doi.org/10.1086/174065)
- Mitsuda, K., Inoue, H., Koyama, K., et al. 1984, *PASJ*, 36, 741
- Mizuno, T., Kubota, A., & Makishima, K. 2001, *ApJ*, 554, 1282, doi: [10.1086/321418](https://doi.org/10.1086/321418)
- Nasa High Energy Astrophysics Science Archive Research Center (Heasarc). 2014, HEASoft: Unified Release of FTOOLS and XANADU, Astrophysics Source Code Library, record ascl:1408.004. <http://ascl.net/1408.004>
- Pakull, M. W., & Mirioni, L. 2002, *arXiv e-prints*, astro, doi: [10.48550/arXiv.astro-ph/0202488](https://doi.org/10.48550/arXiv.astro-ph/0202488)

- Pinto, C., Middleton, M. J., & Fabian, A. C. 2016, *Nature*, 533, 64, doi: [10.1038/nature17417](https://doi.org/10.1038/nature17417)
- Pinto, C., Alston, W., Soria, R., et al. 2017, *MNRAS*, 468, 2865, doi: [10.1093/mnras/stx641](https://doi.org/10.1093/mnras/stx641)
- Pintore, F., Zampieri, L., Stella, L., et al. 2017, *ApJ*, 836, 113, doi: [10.3847/1538-4357/836/1/113](https://doi.org/10.3847/1538-4357/836/1/113)
- Poutanen, J., Lipunova, G., Fabrika, S., Butkevich, A. G., & Abolmasov, P. 2007, *MNRAS*, 377, 1187, doi: [10.1111/j.1365-2966.2007.11668.x](https://doi.org/10.1111/j.1365-2966.2007.11668.x)
- Prestwich, A. H., Tsantaki, M., Zezas, A., et al. 2013, *ApJ*, 769, 92, doi: [10.1088/0004-637X/769/2/92](https://doi.org/10.1088/0004-637X/769/2/92)
- Robba, A., Pinto, C., Walton, D. J., et al. 2021, *A&A*, 652, A118, doi: [10.1051/0004-6361/202140884](https://doi.org/10.1051/0004-6361/202140884)
- Serlemitsos, P. J., Soong, Y., Chan, K.-W., et al. 2007, *PASJ*, 59, S9, doi: [10.1093/pasj/59.sp1.S9](https://doi.org/10.1093/pasj/59.sp1.S9)
- Shakura, N. I., & Sunyaev, R. A. 1973, *A&A*, 24, 337
- Shimura, T., & Takahara, F. 1995, *ApJ*, 445, 780, doi: [10.1086/175740](https://doi.org/10.1086/175740)
- Soria, R., & Kong, A. 2016, *MNRAS*, 456, 1837, doi: [10.1093/mnras/stv2671](https://doi.org/10.1093/mnras/stv2671)
- Thuan, T. X., Bauer, F. E., Papaderos, P., & Izotov, Y. I. 2004, *ApJ*, 606, 213, doi: [10.1086/382949](https://doi.org/10.1086/382949)
- Thuan, T. X., & Martin, G. E. 1981, *ApJ*, 247, 823, doi: [10.1086/159094](https://doi.org/10.1086/159094)
- Uchiyama, Y., Maeda, Y., Ebara, M., et al. 2008, *PASJ*, 60, S35, doi: [10.1093/pasj/60.sp1.S35](https://doi.org/10.1093/pasj/60.sp1.S35)
- Urquhart, R., & Soria, R. 2016, *MNRAS*, 456, 1859, doi: [10.1093/mnras/stv2293](https://doi.org/10.1093/mnras/stv2293)
- Virtanen, P., Gommers, R., Oliphant, T. E., et al. 2020, *Nature Methods*, 17, 261, doi: [10.1038/s41592-019-0686-2](https://doi.org/10.1038/s41592-019-0686-2)
- Walton, D. J., Mackenzie, A. D. A., Gully, H., et al. 2022, *MNRAS*, 509, 1587, doi: [10.1093/mnras/stab3001](https://doi.org/10.1093/mnras/stab3001)
- Walton, D. J., Fürst, F., Heida, M., et al. 2018, *ApJ*, 856, 128, doi: [10.3847/1538-4357/aab610](https://doi.org/10.3847/1538-4357/aab610)
- Watarai, K.-y., & Fukue, J. 1999, *PASJ*, 51, 725, doi: [10.1093/pasj/51.5.725](https://doi.org/10.1093/pasj/51.5.725)
- Watarai, K.-y., Fukue, J., Takeuchi, M., & Mineshige, S. 2000, *PASJ*, 52, 133, doi: [10.1093/pasj/52.1.133](https://doi.org/10.1093/pasj/52.1.133)
- Watarai, K.-Y., & Mineshige, S. 2001, *PASJ*, 53, 915, doi: [10.1093/pasj/53.5.915](https://doi.org/10.1093/pasj/53.5.915)
- Wiktorowicz, G., Sobolewska, M., Lasota, J.-P., & Belczynski, K. 2017, *ApJ*, 846, 17, doi: [10.3847/1538-4357/aa821d](https://doi.org/10.3847/1538-4357/aa821d)
- Zampieri, L., & Roberts, T. P. 2009, *MNRAS*, 400, 677, doi: [10.1111/j.1365-2966.2009.15509.x](https://doi.org/10.1111/j.1365-2966.2009.15509.x)
- Zwicky, F. 1966, *ApJ*, 143, 192, doi: [10.1086/148490](https://doi.org/10.1086/148490)